chemosensors

MDPI

Article

Adsorptive Stripping Voltammetric Determination of Germanium(IV) at a Mercury-Free Bismuth Film Electrode Using Quercetin: Substituent Effect of the 5′-Sulfonate Group on Complex Adsorption and Analytical Sensitivity

Diego Escobar-Olivos [1], Simón Castro-Volpato [1], Paul Jara [1], Marisol Gómez [2] and Carlos Rojas-Romo [1,*]

[1] Facultad de Ciencias, Departamento de Química, Universidad de Chile, Las Palmeras 3425, Santiago 7800024, Chile; diescobar@ug.uchile.cl (D.E.-O.); simon.castro.v@ug.uchile.cl (S.C.-V.); pjara@uchile.cl (P.J.)
[2] Centro de Estudios e Investigación en Salud y Sociedad, Facultad de Ciencias Médicas, Universidad Bernardo O'Higgins, Avenida Placer 1410, Santiago 8361439, Chile; marisol.gomez@ubo.cl
* Correspondence: carlosrojas@uchile.cl

Abstract

The increasing use of germanium in advanced technologies and its potential release into aquatic environments demand sensitive and accessible analytical methods for its determination at trace levels. This work reports the development of an adsorptive stripping voltammetric method for Ge(IV) determination in freshwater samples using an ex situ bismuth film electrode and quercetin as a complexing agent. The stoichiometry of the Ge(IV)–quercetin complex was established as 1:2 by UV-Vis spectrophotometric titration and non-linear least-squares fitting. The effect of the sulfonic substituent was evaluated by comparing quercetin with quercetin-5′-sulfonic acid under otherwise identical conditions. The method was optimized with respect to pH, buffer concentration, ligand concentration, accumulation potential and time, and electrode cleaning conditions. Under optimized conditions, the method exhibited a linear range of 0.23–24.4 μg L^{-1} (3.17–335.9 nmol L^{-1}), a limit of detection of 0.08 μg L^{-1} (1.10 nmol L^{-1}), and a repeatability of 4.41%. The higher sensitivity achieved with quercetin relative to quercetin-5′-sulfonic acid was attributed to the neutral charge of the Ge(IV)–quercetin complex, which favors adsorption at the electrode surface. The method was successfully applied to groundwater, river water, and tap water samples with relative errors below 5.0%, demonstrating its suitability for environmental water analysis.

Keywords: germanium; adsorptive stripping voltammetry; quercetin; sulfonic acid; bismuth electrode; electroanalysis

Check for updates

Received: 23 July 2026
Revised: 4 September 2026
Accepted: 9 September 2026
Published: 14 September 2026

Copyright: © 2026 by the authors. Licensee MDPI, Basel, Switzerland. This article is an open access article distributed under the terms and conditions of the Creative Commons Attribution (CC BY) license.

1. Introduction

The growing deployment of advanced electronics and renewable-energy technologies has driven demand for a group of low-abundance elements collectively termed technologically critical elements (TCEs). Among these, germanium is indispensable as a substrate for high-efficiency photovoltaic cells, fiber-optic components, and radiation detectors. Unlike major industrial metals, germanium is not mined directly but is recovered primarily as a by-product of zinc refining and coal fly-ash processing, making its supply inherently constrained and geopolitically sensitive [1,2].

The rapid expansion of consumer electronics and the inadequate management of electronic waste (e-waste) at end of life have emerged as significant sources of trace-element

contamination in aquatic environments. Improper disposal, including landfilling of unsorted e-waste, allows leaching of technologically critical elements (TCEs) into surface and groundwaters, where their environmental fate and toxicological impact remain poorly understood. Over the past decade, TCEs have been progressively recognized as contaminants of emerging concern, prompting growing interest in their monitoring at environmentally relevant concentrations [3]. Germanium has been reported in natural waters at concentrations ranging from 0.015 to 0.44 μg L^{-1} [4], with values varying according to geological setting, anthropogenic inputs, and water type [5–7]. Currently, neither the World Health Organization nor the US Environmental Protection Agency has established a maximum contaminant level or health-based guideline value for germanium in drinking water, reflecting a gap in regulatory frameworks that underscores the need for sensitive and reliable analytical methods for its environmental monitoring. Speciation studies of germanium in aqueous matrices show that Ge(IV) is the predominant and most stable form, while Ge(II) is readily oxidized to Ge(IV) under naturally occurring oxidizing conditions [8].

Germanium in water samples is typically determined by ICP-OES and ICP-MS, which offer high sensitivity, wide linear ranges, and multielement capability. When coupled with hydride generation and cryogenic trapping, ICP-MS/MS achieves detection limits as low as 0.015 ng L^{-1} for inorganic germanium in water [5]. However, direct ICP-MS determination requires specialized instrumental configurations such as dynamic reaction cells to overcome severe polyatomic interferences on all major Ge isotopes, and ICP-OES is generally not sensitive enough for sub-μg L^{-1} determination in natural waters. In all cases, these techniques require costly instrumentation and high operational expenses, including continuous argon consumption and specialized maintenance. Electroanalytical techniques represent a cost-effective alternative, offering accessible instrumentation, minimal maintenance requirements, portability, and the potential for in situ analysis [9]. Stripping voltammetry combines a preconcentration step with a voltammetric measurement step, enabling the quantification of metal ions at sub-μg L^{-1} concentration levels [10]. During the preconcentration step, the analyte is accumulated on the electrode surface, substantially enhancing the analytical signal obtained in the subsequent voltammetric scan. In adsorptive stripping voltammetry (AdSV), preconcentration is achieved through the adsorption of a metal–ligand complex formed with a suitable organic complexing agent, which is subsequently reduced or oxidized during the stripping step.

The choice of working electrode and complexing agent are two key factors governing the performance of an AdSV method. Historically, mercury-based electrodes dominated trace-metal stripping voltammetry owing to their intrinsic capacity to adsorb electroactive species and their wide cathodic window, which results from the high hydrogen evolution overpotential of mercury. However, the toxicity of mercury has driven the development of alternative electrode materials. Bismuth film electrodes (BiFE) have emerged as one of the most suitable mercury-free alternatives, largely preserving the favorable adsorptive and electrochemical properties of mercury-based electrodes while offering significantly lower toxicity and a greener analytical platform for stripping voltammetric analysis. Unlike bare glassy carbon electrodes, which exhibit limited adsorptive capacity for metal–ligand complexes and a narrower cathodic window in aqueous media, bismuth film electrodes provide a renewable and reproducible surface with adsorptive properties comparable to those of mercury, making them particularly suited for the accumulation of electroactive complexes in AdSV [11–13]. Adsorptive stripping voltammetric methods for Ge(IV) at bismuth film electrodes have been reported by Grabarczyk and Adamczyk, who employed an in situ bismuth film on a glassy carbon substrate with chloranilic acid as the complexing agent, achieving a detection limit of 1.2 nmol L^{-1} [14]. Królicka et al. developed a catalytic approach in which the Ge(IV)–catechol complex was accumulated at ex situ bismuth films

deposited on glassy carbon or screen-printed carbon electrodes, and the analytical signal was enhanced through a catalytic cycle driven by a V(IV)–HEDTA oxidant; detection limits of 0.8 nmol L^{-1} (screen-printed carbon) and 1.0 nmol L^{-1} (glassy carbon) were obtained at an accumulation time of 30 s [15]. More recently, the Grabarczyk group reported a method combining an in situ bismuth film with a carbon nanotubes/spherical glassy carbon electrode and chloranilic acid as a ligand, achieving a detection limit of 0.3 nmol L^{-1} [16].

Quercetin (3,5,7,3′,4′-pentahydroxyflavone) is a polyphenolic flavonol that forms stable, electroactive complexes with a wide range of metal ions and has been used extensively as a complexing and adsorbing ligand in AdSV. Our group has studied quercetin and its sulfonic derivative quercetin-5′-sulfonic acid (QSA) as complexing agents for the simultaneous determination of Sb(III) and Mo(VI) [17], and for the individual determination of Sb(III) [18], V(V) [19], and Mo(VI) [20] at mercury and bismuth electrodes. These works have evidenced that the sulfonic acid group, which does not participate in metal coordination, increases the solubility of the free ligand and modifies the net charge of the complex, reducing competitive adsorption between the ligand and the complex at the electrode surface and thereby increasing the efficiency of the accumulation step. A similar substituent effect has been reported for the determination of Sb(III) using 8-hydroxyquinoline and its sulfonated derivative 8-hydroxyquinoline-5-sulfonic acid, where the presence of the sulfonate group increased the sensitivity of the method by a factor of 2.2 [21]. The application of quercetin to Ge(IV) determination by AdSV has not been previously reported. More importantly, the present work introduces a charge-based rationale for ligand selection in AdSV: by exploiting the neutral character of the Ge(IV)–quercetin complex formed at pH 6.0, efficient electrode accumulation is achieved without catalytic oxidants or chemically modified substrates. This mechanistic framework, systematically evaluated through comparison with QSA, represents the main novelty of the present study.

The aim of the present work is to develop and validate an AdSV method for Ge(IV) determination at an ex situ bismuth film electrode, using the charge-based ligand selection strategy introduced above, and to apply it to the analysis of natural water samples.

2. Materials and Methods

2.1. Instrumentation

Voltammograms were recorded with a Metrohm Autolab PGSTAT204 potentiostat with Nova 2.1 software equipped with an 846 Dosing Interface and a Metrohm 801 magnetic stirrer for solution stirring (all Metrohm, Herisau, Switzerland). A three-electrode configuration was used: a 3.0 mm glassy carbon electrode as the working electrode substrate, a platinum wire auxiliary electrode, and an Ag/AgCl/KCl (3.0 mol L^{-1}) reference electrode (all CH Instruments, Austin, TX, USA). pH was monitored with a Thermo Scientific Orion Star A111 pH meter (Waltham, MA, USA). Water samples were digested using a Metrohm 705 UV digester (Herisau, Switzerland).

2.2. Reagents and Solutions

Working solutions of Ge(IV) were prepared by serial dilution of a 1000 mg L^{-1} stock standard using ultrapure water obtained from a Simplicity® Water Purification System (Merck Millipore, Burlington, MA, USA). Standard solutions of metals and metalloids (1000 mg L^{-1}), Suprapur® acids (nitric, sulfuric, perchloric, phosphoric, boric, acetic), Suprapur® sodium hydroxide (30% solution), sodium acetate, hydrogen peroxide (30%), sodium nitrate, sodium chloride, sodium sulfate, sodium fluoride, EDTA, and CDTA were obtained from Merck (Burlington, MA, USA). Quercetin (3,5,7,3′,4′-pentahydroxyflavone, ≥95% purity) was obtained from Sigma-Aldrich (St. Louis, MO, USA). Quercetin-5′-sulfonic acid was synthesized according to a previously reported procedure [19].

2.3. Bismuth Film Preparation and Voltammetric Procedure

Before each set of measurements, the glassy carbon electrode was polished sequentially with 0.3 μm and 0.05 μm alumina slurry to a mirror finish, rinsed with deionized water, and sonicated for 30 s. The bismuth film was deposited from 10.0 mL of a 150.0 mg L^{-1} Bi(III) solution in 0.5 mol L^{-1} acetate buffer (pH 4.5). The solution was deoxygenated with nitrogen for 5 min, and a deposition potential of −0.8 V was applied for 300 s under stirring. The working electrode was then rinsed with deionized water and transferred to the measuring cell.

All measurements were performed in an initial volume of 10.0 mL, completed with deionized water. The supporting electrolyte was 60 mmol L^{-1} phosphate buffer (pH 6.0) and 5.0 μmol L^{-1} of quercetin. The Ge(IV)–quercetin complex was accumulated at −0.5 V for 30 s under stirring. The stirrer was then stopped, and after a 10 s equilibration period the potential was scanned from −0.5 to −1.1 V by square-wave voltammetry (step potential −4.0 mV, amplitude 25 mV, frequency 15 Hz). After each scan, the electrode was cleaned at −1.2 V for 20 s under stirring. Each measurement was performed in triplicate from the same solution, and the mean peak current was used for quantification.

2.4. Stoichiometry Determination of the Ge(IV)–Quercetin Complex

The stoichiometry of the Ge(IV) quercetin complex was determined by spectrophotometric titration using a Shimadzu UV-1800 spectrophotometer (Kyoto, Japan) at 25 °C and using a 1 cm path length cell. Solutions were prepared in ethanol:water (1:1, *v*/*v*) with 60 mmol L^{-1} phosphate buffer at pH 6.0. The molar extinction coefficient of free quercetin at 415 nm (ε_L = 3715 ± 28 L mol^{-1} cm^{-1}) was determined from a calibration curve (10 to 70 μmol L^{-1}) in the absence of Ge(IV) and treated as a fixed parameter. The total Ge(IV) concentration was held constant at 20.7 μmol L^{-1} while the total quercetin concentration was varied from 0 to 300 μmol L^{-1} across 20 independently prepared solutions. Absorbance was recorded at 415 nm after 10 min, the time required to reach equilibrium as established by kinetic monitoring.

The stoichiometry was determined by fitting the absorbance versus total quercetin concentration data to the equilibrium model $M + nL \rightleftharpoons ML_n$ with global formation constant:

$$\beta_n = [ML_n]/([M][L]^n) \quad (1)$$

The calculated absorbance at each point was:

$$A = \varepsilon_L[L] + \varepsilon_{ML_n}[ML_n] \quad (2)$$

where $[L] = [L]_T - n[ML_n]$. For each point, $[ML_n]$ was obtained by solving the polynomial:

$$\beta_n[L]^{n+1} + \beta_n(n[M]_T - [L]_T)[L]^n + [L] - [L]_T = 0 \quad (3)$$

using the Newton-Raphson method with an analytical derivative, typically converging in 3 to 4 iterations. The free parameters $\log_{10}(\beta_n)$, ε_{ML_n}, and an instrumental offset were optimized by minimizing the sum of squared residuals using the GRG nonlinear solver (Microsoft Excel, Microsoft 365, version 2608). Each model was run from multiple starting points to avoid local minima, and the solution with the lowest residual sum was retained. Fitting was performed independently for the ML_1, ML_2, and ML_3 models.

2.5. Water Sample Analysis

Natural water samples were collected in October 2025 from three sources: groundwater from Batuco (Santiago Metropolitan Region), river water from the Bío-Bío River (Bío-Bío

Region), and tap water from the Ñuñoa domestic network (Santiago Metropolitan Region). Samples were collected in acid-washed polyethylene bottles, filtered through a 0.45 μm membrane, and stored at 4 °C prior to digestion. Prior to analysis, 9.5 mL aliquots were digested with 30% hydrogen peroxide (500 μL) under UV irradiation at 96–98 °C for 120 min to remove organic matter. Digested samples were analyzed within 48 h of digestion; remaining aliquots were divided into 25.0 mL fractions and stored at −18 °C for future use. Samples were spiked with 5.0 μg L^{-1} Ge(IV), and quantification was performed by the standard addition method to compensate for matrix effects.

3. Results and Discussion

The preparation of ex situ bismuth film electrodes has been widely studied, and different deposition procedures have been reported. Previous work from our group established that a 0.5 mol L^{-1} acetate buffer (pH 4.5) with a Bi(III) concentration between 100.0 and 150.0 mg L^{-1}, a deposition potential of −0.8 V, and a deposition time between 300 and 600 s represent suitable conditions for bismuth film formation on carbon substrates [20,22]. On this basis, the Bi(III) concentration and deposition time were optimized at a fixed deposition potential of −0.8 V. Unless otherwise stated, the following preliminary conditions were used during optimization: 50.0 mmol L^{-1} phosphate buffer (pH 5.0), 15.0 μmol L^{-1} quercetin, accumulation potential −0.4 V, accumulation time 60 s, and 30.0 μg L^{-1} Ge(IV).

3.1. Optimization of Bi(III) Concentration and Deposition Time for Bismuth Film Preparation

Three Bi(III) concentrations (50.0, 100.0, and 150.0 mg L^{-1}) and three deposition times (150, 300, and 600 s) were combined to evaluate the effect of both variables on the reduction signal of the Ge(IV)–quercetin complex and the repeatability, expressed as the relative standard deviation (RSD) of 15 consecutive measurements in the same solution.

Figure 1 shows the effect of both parameters on the analytical response; error bars represent the standard deviation of the measurement set. For Bi(III) concentrations of 50.0 and 100.0 mg L^{-1} at deposition times of 150 and 300 s, no analytical signal was observed. A measurable response required a deposition time of 600 s at all three Bi(III) concentrations, with the analytical response increasing with Bi(III) concentration. The maximum response was achieved at 150.0 mg L^{-1} Bi(III) and 600 s, but the RSD of consecutive measurements was 22%. At this deposition time, partial detachment of the bismuth film from the electrode substrate was observed during the stirring step, a phenomenon that has been previously described for ex situ bismuth films [20] and that accounts for the high variability of the analytical responses. The best balance between signal intensity and measurement stability was obtained at 150.0 mg L^{-1} Bi(III) and a deposition time of 300 s, which yielded an RSD of 7%. Therefore, the bismuth film was deposited from a 0.5 mol L^{-1} acetate buffer solution (pH 4.5) containing 150.0 mg L^{-1} Bi(III) at −0.8 V for 300 s in all subsequent experiments.

3.2. Optimization of Accumulation and Cleaning Conditions

The composition and physicochemical properties of the supporting electrolyte govern the efficiency of the metal–complex accumulation step at the electrode surface. The following experimental variables were optimized to maximize the analytical response: pH, supporting electrolyte composition and concentration, complexing agent concentration, accumulation potential and time, and cleaning potential and time. Optimization studies were conducted using Q as the complexing agent. The effect of the sulfonic substituent on the efficiency of complex accumulation and the competitive adsorption between the free ligand and the complex at the electrode surface was evaluated by comparing Q and QSA in the ligand concentration optimization study.

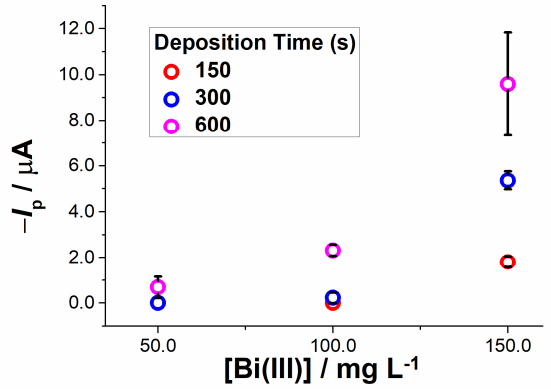


Figure 1. Effect of Bi(III) concentration and deposition time on the reduction signal of the Ge(IV)–Q complex. BiFE preparation conditions: 0.5 mol L^{-1} acetate buffer (pH 4.5); E_{dep}: −0.8 V. Measurement conditions: 50.0 mmol L^{-1} phosphate buffer (pH 5.0); E_{acc}: −0.4 V; t_{acc}: 60 s; [Ge(IV)]: 30.0 μg L^{-1}; [Q]: 15.0 μmol L^{-1}.

3.2.1. Effect of pH, Supporting Electrolyte Composition, and Concentration

The effect of pH on the analytical response of the Ge(IV)–Q complex was studied using Britton–Robinson (BR) buffer in the pH range 2.9–7.3, adjusted by the addition of 2 mol L^{-1} NaOH. As shown in Figure 2, the maximum peak current and best signal symmetry were obtained at pH 6.0, which was selected as the optimal pH for further studies. At acidic pH values, the hydroxyl groups of quercetin remain protonated, preventing efficient complex formation with Ge(IV); complex formation is favored near pH 6.0, where the most acidic hydroxyl group (C4′-OH, pKa 6.41) approaches deprotonation [23]. At higher pH values, the predominant Ge(IV) species in aqueous solution shifts from the neutral form H_4GeO_4 toward the anionic species $H_3GeO_4^-$ and $H_2GeO_4^{2-}$, and the formation of germanium hydroxides of lower solubility is favored, reducing the availability of Ge(IV) for complex formation [24]. The combination of these two effects defines pH 6.0 as the optimal condition for Ge(IV)–Q complex formation and adsorption at the bismuth film electrode.

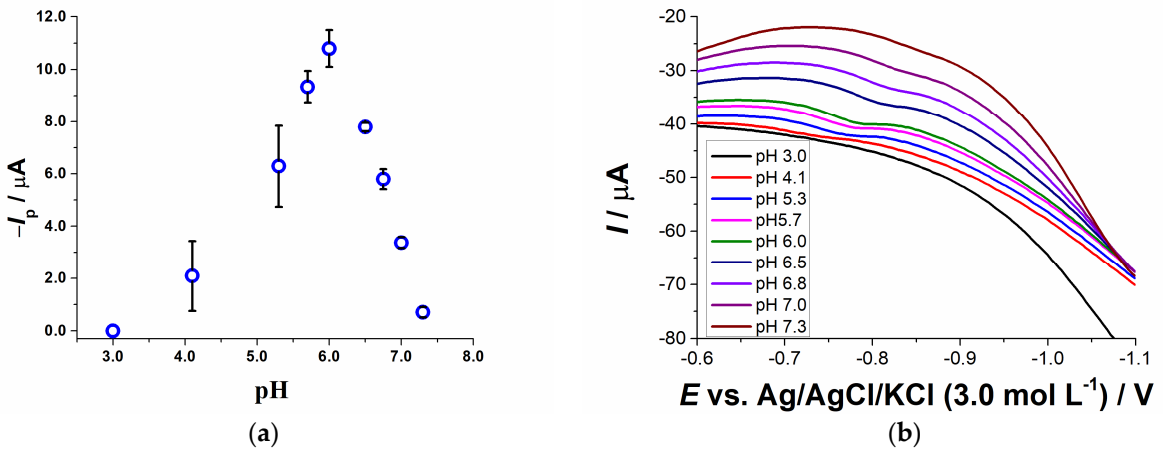


Figure 2. Effect of pH on the reduction signal of the Ge(IV)–Q complex. (**a**) Analytical response and (**b**) Square wave voltammograms. BiFE preparation conditions: 0.5 mol L^{-1} acetate buffer (pH 4.5); E_{dep}: −0.8 V; t_{dep}: 300 s. Measurement conditions: 50.0 mmol L^{-1} Britton–Robinson buffer; E_{acc}: −0.4 V; t_{acc}: 60 s; [Ge(IV)]: 30.0 μg L^{-1}; [Q]: 15.0 μmol L^{-1}.

The effect of phosphate buffer concentration on the analytical response was subsequently studied at pH 6.0 by the consecutive addition of aliquots of a concentrated phosphate buffer stock solution to the electrochemical cell. As shown in Figure 3, the analytical response increased with buffer concentration up to 60 mmol L^{-1}, above which

a decrease in peak current and an increase in the standard deviation of consecutive measurements were observed. The decrease at higher buffer concentrations is likely associated with changes in the double layer structure at elevated ionic strength, which may affect the adsorption efficiency of the Ge(IV)–quercetin complex at the electrode surface. A phosphate buffer concentration of 60 mmol L^{-1} at pH 6.0 was therefore selected for all subsequent experiments.

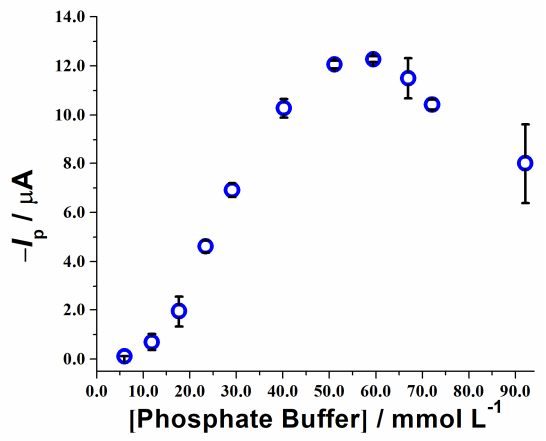


Figure 3. Effect of phosphate buffer concentration on the reduction signal of the Ge(IV)–Q complex. Measurement conditions: pH: 6.0. Other conditions as in Figure 2.

3.2.2. Effect of Complexing Agent Concentration and Substituent on the Analytical Response

Figure 4 shows the peak current as a function of ligand concentration for Q and QSA. Both ligands promote complex formation with Ge(IV) and produce an increase in the analytical signal, confirming their role as complexing and accumulating agents. Q (5.0 μmol L^{-1}) yielded a higher maximum peak current than QSA, while QSA showed a more gradual signal decrease at concentrations beyond the optimum, allowing the use of a wider ligand concentration range without significant sensitivity loss. Based on its higher analytical response, Q was selected as the complexing agent for subsequent method development.

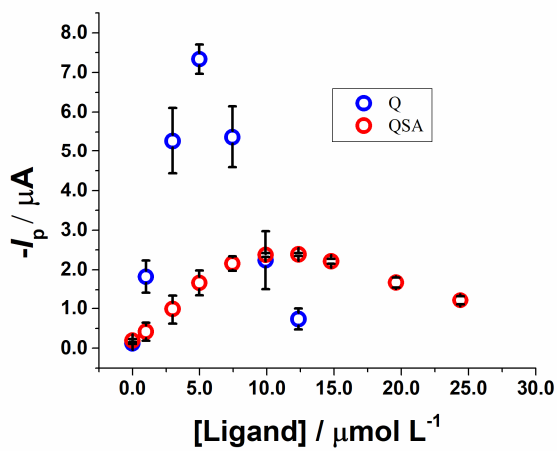


Figure 4. Effect of Q and QSA concentration on the reduction signal of the Ge complexes. Measurement conditions: 60.0 mmol L^{-1} phosphate buffer (pH 6.0). Other conditions as in Figure 2.

To establish the stoichiometry of the Ge(IV)–Q complex, UV-Vis spectrophotometric titrations were performed at 415 nm, keeping $[M]_T$ = 20.7 μmol L^{-1} constant while varying $[L]_T$ from 0 to 300 μmol L^{-1} across 20 independently prepared solutions. Three equilibrium models were evaluated: 1:1, 1:2, and 1:3. The experimental data and fitted curves for

each model are provided in the Supplementary Material (Figures S1–S3). The 1:1 model yielded a substantially lower R^2 and higher sum of squared residuals (SSR) than the remaining models, indicative of structural misfit. The 1:3 model produced R^2 and SSR values comparable to those of 1:2, but the corresponding $\log_{10}(\beta_3) > 13$ is physically unrealistic for a Ge(IV)–flavonoid complex under the present conditions. The 1:2 model was therefore selected, yielding $\log_{10}(\beta_2) = 8.95 \pm 0.14$, $\varepsilon_{ML2} = (46.9 \pm 2.0) \times 10^3$ L mol^{-1} cm^{-1}, and $R^2 = 0.9977$ (Table 1).

Table 1. Fitting parameters obtained from non-linear least-squares analysis of the UV-Vis spectrophotometric titration data for the Ge(IV)–quercetin system under the ML_1, ML_2, and ML_3 equilibrium models.

Parameter	ML_1 (1:1)	ML_2 (1:2)	ML_3 (1:3)
$\log_{10}(\beta)$	4.23 ± 0.26	8.95 ± 0.14	13.85 ± 0.13
ε_{MLn} (10^3 L mol^{-1} cm^{-1})	57.7 ± 8.2	46.9 ± 2.0	47.7 ± 1.0
R^2	0.9883	0.9977	0.9993
SSR	0.0781	0.0155	0.0049

Conditions: λ = 415 nm, $[M]_T$ = 20.7 µmol L^{-1}, $\varepsilon_L = (3.715 \pm 0.028) \times 10^3$ L mol^{-1} cm^{-1}, pH 6.0, ethanol:water 1:1 v/v, 25 °C.

The 1:2 stoichiometry is consistent with the solid-state complex $[C_{30}H_{18}O_{14}Ge]\cdot 2H_2O$ reported by Zhai et al. [25], in which two quercetin molecules coordinate Ge(IV) through the 4C=O and 3C–O chelation site, as confirmed by ^{1}H NMR and thermogravimetric analysis. A 1:2 metal-to-ligand ratio has similarly been reported for quercetin complexes with Fe(III) [26,27], Zr(IV) [28], and Cu(II) under basic conditions [29], reflecting the bidentate character of the 3-OH/4-carbonyl chelation site and its suitability for coordination with higher-valence metal ions.

The higher analytical signal observed with Q relative to QSA can be rationalized based on the net charge of the respective Ge(IV)–ligand complexes. At pH 6.0, Ge(IV) exists predominantly as the neutral species $Ge(OH)_4$ in aqueous solution [30]. Coordination of two quercetin molecules through the deprotonated 3-OH and 4C=O sites, with retention of the two remaining OH^- ligands, yields a net neutral Ge(IV)–Q_2 complex that adsorbs efficiently at the bismuth film electrode surface during accumulation. In the Ge(IV)–QSA_2 system, the sulfonic groups remain uncoordinated and fully deprotonated at pH 6.0, conferring an anionic character to the complex and reducing its affinity for the electrode. Simultaneously, the sulfonic substituent increases the aqueous solubility of free QSA, attenuating competitive adsorption by the excess ligand and explaining the more gradual signal decrease observed at higher QSA concentrations. This behavior contrasts with that reported for Sb(III) and V(V), where the reduced competitive adsorption by free QSA more than compensates for the lower complex accumulation, resulting in higher sensitivity with QSA than with Q [18,19].

These results demonstrate that the charge state of the Ge(IV)–ligand complex is a key factor governing the analytical response in AdSV, and that the advantage of sulfonic flavonoid derivatives over their unsulfonated counterparts is not universal but depends on the specific coordination chemistry of the target analyte. To our knowledge, this is the first study to systematically compare Q and QSA for the voltammetric determination of Ge(IV), providing a mechanistic basis for rational ligand selection as a strategy to optimize sensitivity in adsorptive stripping methods.

3.2.3. Effect of Accumulation Potential and Time

Figure 5a shows the dependence of the analytical signal on the accumulation potential in the range −0.4 to −1.0 V. At potentials more negative than −0.7 V, the signal decreases

sharply because complex reduction competes with adsorption at the electrode surface. An accumulation potential of −0.5 V was selected as optimum. Figure 5b shows the effect of accumulation time on the peak current in the range 0 to 120 s. The signal increased during the first 30 s as the Ge(IV)–Q complex adsorbed at the bismuth film electrode, reached a plateau, and then declined at longer times, likely due to competitive adsorption of excess free quercetin at the electrode surface. An accumulation time of 30 s was therefore selected. Both studies were performed at a Ge(IV) concentration of 10.0 µg L^{-1}, lower than that used in previous optimization steps (30.0 µg L^{-1}), to evaluate the method performance under more challenging analytical conditions.

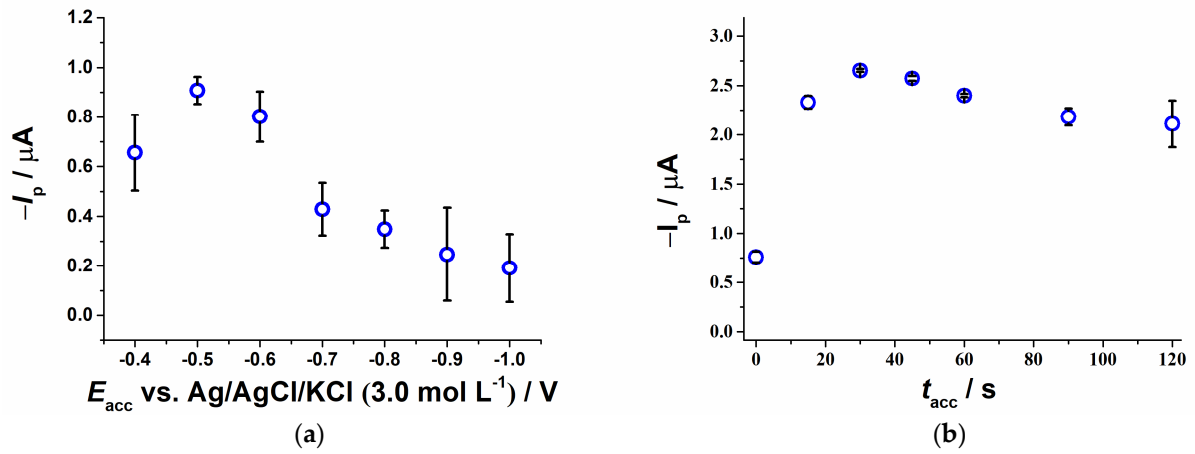


Figure 5. (**a**) Effect of accumulation potential on the analytical response. Measurement conditions: 60.0 mmol L^{-1} phosphate buffer (pH 6.0); t_{acc}: 60 s; [Ge(IV)]: 10.0 µg L^{-1}; [Q]: 5.0 µmol L^{-1}. (**b**) Effect of accumulation time on the analytical response. Measurement conditions: 60.0 mmol L^{-1} phosphate buffer (pH 6.0); E_{acc}: −0.5 V; [Ge(IV)]: 10.0 µg L^{-1}; [Q]: 5.0 µmol L^{-1}. BiFE preparation conditions as in Figure 2.

3.2.4. Electrode Cleaning Step

Under optimal conditions, an electrochemical cleaning step was evaluated to improve measurement repeatability across a set of replicate measurements (n = 10). First, the cleaning potential was varied in the range −1.0 to −1.4 V using a fixed cleaning time of 5 s. A potential of −1.2 V produced the smallest signal decrease while maintaining comparable RSD values across the range studied (Figure 6a). Cleaning time was then optimized at −1.2 V by evaluating times from 5 to 30 s (Figure 6b). A cleaning time of 20 s was selected as optimal because it achieved the lowest RSD despite a reduction in signal intensity relative to shorter cleaning times, improving measurement precision across the replicate set.

3.3. Interference Studies and Analytical Performance

The interference of metal and metalloid ions is one of the most common challenges in the development of an analytical method. A common strategy to reduce their effect is the addition of masking agents to the supporting electrolyte. Three masking agents (EDTA, CDTA, and F^-) were evaluated by determining the maximum concentration that did not produce a signal variation greater than ±10% relative to the unmasked Ge(IV) response, and by measuring the signal variation at a fixed concentration of 480.0 µmol L^{-1}. Table 2 summarizes the results for a 5.0 µg L^{-1} Ge(IV) solution. The maximum tolerable concentrations of EDTA, CDTA, and F^- were selected for inclusion in the supporting electrolyte to minimize interference from co-existing metal and metalloid ions.

Table 2. Effect of masking agent concentration on the Ge(IV) analytical response.

Masking Agent (MA)	[MA] (μmol L^{-1}) (ΔI_p < ±10%)	ΔI_p ([MA] = 480.0 μmol L^{-1})
EDTA	450.0	−11.1
CDTA	60.0	−47.2
F^-	480.0	−6.2

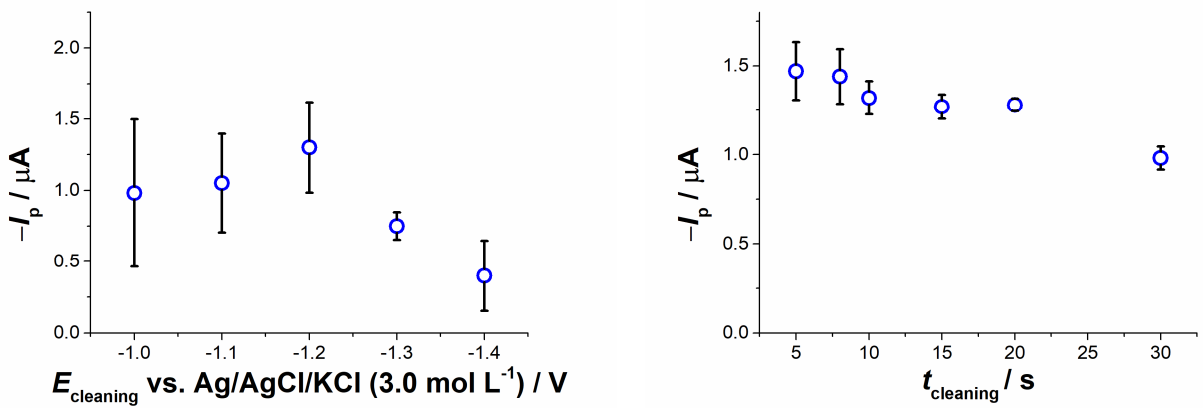


Figure 6. Optimization of the cleaning step conditions. Effect of cleaning potential (**a**) and cleaning time (**b**) on the analytical signal and RSD for replicate measurements (n = 10) under optimal conditions.

The effect of nitrate, sulfate, and chloride (anions commonly present in natural water samples) was evaluated using the same criterion (Table 3) at a maximum concentration of 5.0 mmol L^{-1} and a Ge(IV) concentration of 5.0 μg L^{-1}. Chloride did not affect the analytical signal significantly (ΔI_p < 4% at 5.0 mmol L^{-1}). Sulfate caused a signal decrease of 21.7% at the maximum concentration studied, with a tolerance limit of 4.0 mmol L^{-1}. Nitrate produced the largest interference, with a 36.3% signal decrease at 5.0 mmol L^{-1} and a tolerance limit of 1.0 mmol L^{-1}.

Table 3. Effect of nitrate, sulfate, and chloride concentration on the Ge(IV) analytical response.

Anion	[Anion] (mmol L^{-1}) (ΔI_p < ±10%)	ΔI_p ([Anion] = 5.0 mmol L^{-1})
NO_3^-	1.0	−36.3
SO_4^{2-}	4.0	−21.7
Cl^-	5.0	−3.6

Twenty-two metal and metalloid ions were evaluated as potential interferents in the presence of the selected masking agents. The results, summarized in Table 4, reveal three distinct tolerance levels. Eleven species (Te(VI), Ni(II), Co(II), Ag(I), Li(I), Ga(III), Na(I), In(III), Cd(II), Al(III), and Cr(III)) did not produce signal variations greater than ±10% up to ratios of 100:1 to 500:1. These species are therefore considered non-interfering under the present conditions. A second group comprising Tl(I), Sn(IV), V(V), Pb(II), Cu(II), Hg(II), and Cr(VI) showed moderate interference, with tolerance limits between 25:1 and 100:1.

Four species (Se(IV), Mo(VI), Sb(III), and As(V)) were identified as significant interferents, producing signal suppression exceeding 10% at ratios as low as 2.5:1 to 10:1. Nevertheless, the typical concentrations of these elements in natural waters are considerably lower than the interference thresholds determined in this work. Selenium concentrations in river water are typically in the range 0.02–0.5 μg L^{-1}, with values rarely exceeding 1 μg L^{-1} in uncontaminated surface waters [31]. Molybdenum concentrations in most freshwaters are less than 10 μg L^{-1}, and often orders of magnitude below this value, although elevated concentrations have been reported in areas affected by mining or geothermal activity [32].

Background antimony concentrations in surface waters are typically around 0.1 μg $L^{-1,}$ and arsenic baseline concentrations in river water generally range from 0.1 to 0.8 μg L^{-1} in unpolluted systems, although elevated levels are found in areas affected by geothermal activity or mining [33]. Given that these environmental concentrations are substantially below the interference thresholds established here, a specific removal protocol is not considered necessary for the analysis of natural water samples under typical conditions.

Table 4. Effect of potentially interfering metal and metalloid ions on the Ge(IV) analytical signal.

Interferent	[Int]:[Ge(IV)] (ΔI_p < ±10%)	%ΔI_p [Int]:[Ge(IV)] 500:1	Interferent	[Int]:[Ge(IV)] (ΔI_p < ±10%)	%ΔI_p [Int]:[Ge(IV)] 500:1
Se(IV)	2.5	−100	Al(III)	100	−11.9
Mo(VI)	2.5	−100	Cr(III)	250	−19.8
Sb(III)	5	−100	Cd(II)	500	0
As(V)	10	−14.2	Te(VI)	500	0
Tl(I)	25	−55.2	Ni(II)	500	0
Sn(IV)	25	−37.2	Co(II)	500	0
V(V)	25	−15.2	Ag(I)	500	0
Pb(II)	50	−14.2	Li(I)	500	0
Cu(II)	50	−34.9	Ga(III)	500	0
Hg(II)	100	−42.4	Na(I)	500	0
Cr(VI)	100	−35.1	In(III)	500	0

5.0 μg L^{-1} Ge(IV), supporting electrolyte containing 450.0 μmol L^{-1} EDTA, 60.0 μmol L^{-1} CDTA, and 480.0 μmol L^{-1} fluoride.

Among the interferents identified, Mo(VI) warrants particular attention. Unlike the others, Mo(VI) generates an electrochemical signal at a potential very close to that of Ge(IV), causing progressive signal suppression at low Mo(VI):Ge(IV) ratios and complete peak overlap at higher concentrations (Figure S4). This signal proximity makes Mo(VI) the most analytically challenging interferent, particularly in matrices where Mo concentrations may approach or exceed those of Ge(IV). The development of a selective masking or separation strategy for Mo(VI) is therefore recommended as a priority for future work.

Under optimized conditions for bismuth film deposition: 150.0 μg L^{-1} Bi(III), deposition potential and time of −0.8 V and 300 s, respectively; measurement conditions: 60.0 mmol L^{-1} phosphate buffer (pH 6.0) in the presence of EDTA, CDTA and fluoride, accumulation potential and time of −0.4 V and 30 s, respectively, 5.0 μmol L^{-1} quercetin and cleaning potential and time of −1.2 V and 20 s, respectively. A calibration plot for Ge(IV) was constructed (Figure 7) between 1.0 and 24.4 μg L^{-1}. A linear relationship between peak current and Ge(IV) concentration was obtained across the entire studied concentration range and described by the regression equation I_p (μA) = 0.173 [Ge(IV)] (μA L μg^{-1}) − 0.095 (μA), with a correlation coefficient of R^2 = 0.999. The limit of detection (LOD) and limit of quantification (LOQ) were calculated as LOD = $3.3s_B/m$ and LOQ = $10s_B/m$, where s_B is the standard deviation of the intercept and m is the slope of the calibration curve, yielding LOD = 0.08 μg L^{-1} (1.10 nmol L^{-1}) and LOQ = 0.23 μg L^{-1} (3.17 nmol L^{-1}).

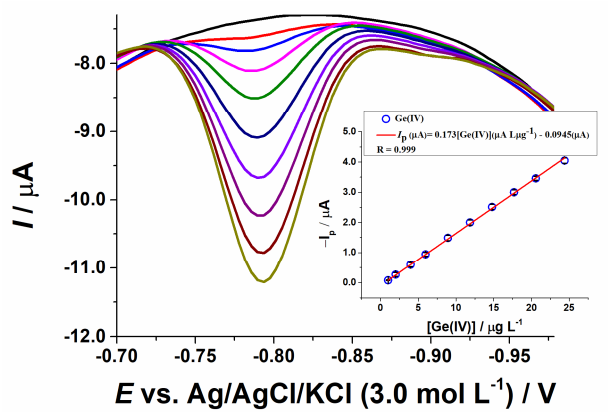


Figure 7. Voltammograms for increasing Ge(IV) concentrations and Ge(IV) calibration plot (inset). BiFE preparation conditions: 0.5 mol L^{-1} acetate buffer (pH 4.5); E_{dep}: −0.8 V; t_{dep}: 300 s. Measurement conditions: 60.0 mmol L^{-1} phosphate buffer (pH 6.0); 450.0 µmol L^{-1} EDTA; 60.0 µmol L^{-1} CDTA; 480.0 µmol L^{-1} fluoride; [Q]: 5.0 µmol L^{-1}; E_{acc}: −0.5 V; t_{acc}: 30 s. Electrode cleaning conditions: E_{clean}: −1.2 V; t_{clean}: 20 s.

The repeatability of the method, expressed as RSD and determined from 15 consecutive measurements of the same solution and electrode, was 4.41%. The reproducibility, expressed as RSD and determined from 20 measurements performed with different solutions and freshly deposited bismuth film electrodes under optimal conditions and a Ge(IV) concentration of 5.0 µg L^{-1}, was 12.2%.

Table 5 compares the analytical performance of the present method with the three AdSV procedures reported in the literature for the determination of Ge(IV) at bismuth film electrodes. The LOD obtained in this work (1.10 nmol L^{-1}) is competitive with those reported by Grabarczyk and Adamczyk [14] (1.2 nmol L^{-1}) and by Królicka et al. [15] (0.8–1.0 nmol L^{-1}) at equivalent accumulation times of 30 s. A lower LOD of 0.3 nmol L^{-1} was achieved by Grabarczyk and Adamczyk [16] using a carbon nanotube-modified electrode, demonstrating the potential of advanced electrode substrates for further sensitivity improvement. The linear range of the present method (3.17–335.9 nmol L^{-1}) extends to higher concentrations than those reported by Grabarczyk and Adamczyk [14] (3.0–150 nmol L^{-1}), Królicka et al. [15] (1.5–24 nmol L^{-1}), and Grabarczyk and Adamczyk [16] (0.9–30 nmol L^{-1}), which is advantageous for the direct analysis of samples with variable Ge(IV) content without requiring prior dilution.

A different electrochemical approach for germanium determination using a nanoporous gold electrode has been recently reported by Rojas et al. [34], based on the anodic stripping of electrodeposited Ge(II) rather than the cathodic reduction of an adsorbed Ge(IV)–ligand complex. This method achieved a LOD of 21.1 nmol L^{-1} (1.53 µg L^{-1}) and a linear range of 138–551 nmol L^{-1} (10–40 µg L^{-1}) for Ge(II). Gold has also been explored as a substrate for bismuth film deposition in AdSV of Ge(IV): Królicka et al. [15] evaluated bismuth-coated gold electrodes (Bi/Au) and found performance comparable to bismuth-coated glassy carbon, indicating that the electroactive surface in both cases is the bismuth film rather than the underlying substrate. Although the analyte oxidation state and electrochemical mechanism differ from the present work, these reports further illustrate the growing interest in mercury-free electrode platforms for germanium determination.

A distinguishing feature of the present method is the rational selection of quercetin as a complexing agent based on the net charge of the Ge(IV)–ligand complex. By exploiting the coordination chemistry of Ge(IV) with flavonoid ligands to generate a neutral complex, efficient adsorption at the electrode surface is achieved without the need for a catalytic oxidant system, as required by Królicka et al. [15], or a specialized carbon nanotube

substrate, as employed by Grabarczyk and Adamczyk [16]. This ligand selection strategy, based on matching the complex charge to the electrode adsorption requirements, represents a general framework that could guide the development of improved AdSV methods for other metal ions and could be further exploited in combination with carbon nanomaterial-modified electrodes to achieve lower detection limits.

Table 5. Comparison of AdSV methods for the determination of Ge(IV) at bismuth film electrodes.

Electrode	Ligand	Technique	t_{acc} (s) [a]	Linear Range (nmol L^{-1})	LOD (nmol L^{-1})	Ref.
BiFE in situ/GCE	Chloranilic acid	DPV	50	3.0–150	1.2	[14]
BiFE ex situ/SPE	Catechol + V(IV)–HEDTA	cAdSV	30	1.5–19.5	0.8	[15]
BiFE ex situ/GCE	Catechol + V(IV)–HEDTA	cAdSV	30	1.5–24	1.0	[15]
BiFE in situ/CNTs/SGCE	Chloranilic acid	AdSV	40	0.9–30	0.3	[16]
BiFE ex situ/GCE	Quercetin	SWV	30	3.17–336	1.10	This work
NPG	-	SWASV [Ge(II)] [b]	210	138–551	21.1	[34]

[a] For in situ BiFE, t_{acc} corresponds to the sum of the bismuth film deposition time and the Ge(IV) complex accumulation time. [b] Method based on anodic stripping of electrodeposited Ge(II); not directly comparable to AdSV methods for Ge(IV). AdSV: adsorptive stripping voltammetry; BiFE: bismuth film electrode; cAdSV: catalytic adsorptive stripping voltammetry; CNTs/SGCE: carbon nanotubes/spherical glassy carbon electrode; DPV: differential pulse voltammetry; GCE: glassy carbon electrode; NPG: nanoporous gold film; SPE: screen-printed carbon electrode; SWASV: square wave anodic stripping voltammetry; SWV: square wave voltammetry.

3.4. Application of the Methodology

The applicability of the method was evaluated by the analysis of three freshwater samples: groundwater, river water (Figure S5), and tap water. The samples were digested using an H_2O_2/UV method to eliminate organic matter. Ge(IV) was not detected in any of the analyzed samples, with concentrations below the LOD of the method. The samples were spiked with 5.0 μg L^{-1} of Ge(IV) and analyzed by the standard addition method, with relative errors below 5.0% for all samples. The results are summarized in Table 6.

Table 6. Application of the developed methodology in the analysis of freshwater samples.

Freshwater Sample	Determined [Ge(IV)] in the Sample (μg L^{-1})	Determined [Ge(IV)] in the Spiked Sample ± SD (μg L^{-1})	Relative Error (%)
Batuco groundwater	ND	5.10 ± 0.02	2.0
Bío Bio River water	ND	4.84 ± 0.05	−3.2
Tap water	ND	4.95 ± 0.23	−1.0

ND: Not detected; SD: Standard deviation.

4. Conclusions

The present work demonstrates that rational ligand selection based on the net charge of the metal–ligand complex is a key strategy for the development of sensitive AdSV methods. The Ge(IV)–quercetin 1:2 complex, formed at pH 6.0 through coordination with $Ge(OH)_4$, carries a net neutral charge that favors efficient adsorption at the bismuth film electrode, yielding an LOD of 0.08 μg L^{-1} (1.10 nmol L^{-1}) and a linear range of 0.23–24.4 μg L^{-1} (3.17–335.9 nmol L^{-1}) with analytical performance competitive with

previously reported methods. The comparison with quercetin-5′-sulfonic acid confirms that the sulfonic substituent, while advantageous for other metals, reduces sensitivity for Ge(IV) by conferring anionic character to the complex. The applicability of the method was demonstrated through the successful determination of Ge(IV) in three freshwater samples. These findings suggest a mechanistic framework for ligand selection in AdSV that is extendable to other metal ions and electrode platforms. The combination of this charge-based ligand selection strategy with carbon nanomaterial-modified electrodes and the exploration of structurally related neutral-complex-forming flavonoid ligands are proposed as priorities for future work.

Supplementary Materials: The following supporting information can be downloaded at https://www.mdpi.com/article/10.3390/chemosensors14090204/s1, Figure S1: Evaluation of the stoichiometry of the Ge(IV)–quercetin complex by UV-Vis spectrophotometric titration at 415 nm using the ML_1 (1:1) equilibrium model; Figure S2: Evaluation of the stoichiometry of the Ge(IV)–quercetin complex by UV-Vis spectrophotometric titration at 415 nm using the ML2 (1:2) equilibrium model. (○) Experimental absorbance; (—) theoretical absorbance calculated from the model; Figure S3: Evaluation of the stoichiometry of the Ge(IV)–quercetin complex by UV-Vis spectrophotometric titration at 415 nm using the ML_3 (1:3) equilibrium model; Figure S4: Effect of Mo(VI) on the Ge(IV) analytical signal showing progressive signal suppression and peak overlap at increasing Mo(VI):Ge(IV) ratios; Figure S5: Square wave voltammograms obtained for the Bío-Bío River water sample showing the unspiked sample, the spiked sample, and successive standard additions.

Author Contributions: Conceptualization, C.R.-R.; methodology, D.E.-O. and C.R.-R.; validation, D.E.-O., S.C.-V. and C.R.-R.; formal analysis, D.E.-O., S.C.-V., P.J. and C.R.-R.; investigation, D.E.-O., S.C.-V., M.G., P.J. and C.R.-R.; resources, P.J. and C.R.-R.; data curation, D.E.-O., S.C.-V., M.G. and C.R.-R.; writing—original draft preparation, C.R.-R.; writing—review and editing, D.E.-O., S.C.-V., M.G., P.J. and C.R.-R.; visualization, D.E.-O., S.C.-V. and C.R.-R.; supervision, C.R.-R.; project administration, C.R.-R.; funding acquisition, C.R.-R. All authors have read and agreed to the published version of the manuscript.

Funding: This research was funded by Agencia Nacional de Investigación y Desarrollo: Proyecto Iniciacion 11240755.

Institutional Review Board Statement: Not applicable.

Informed Consent Statement: Not applicable.

Data Availability Statement: The data that support the findings of this study are available on request from the corresponding author.

Acknowledgments: During the preparation of this manuscript, the authors used Claude AI (Sonnet 4.6) for orthographic revision and writing assistance. The authors have reviewed and edited the output and take full responsibility for the content of this publication.

Conflicts of Interest: The authors declare no conflicts of interest.

Abbreviations

The following abbreviations are used in this manuscript:

AdSV	Adsorptive stripping voltammetry
BiFE	Bismuth film electrode
BR	Britton-Robinson
cAdSV	Catalytic adsorptive stripping voltammetry
CNTs/SGCE	Carbon nanotubes/spherical glassy carbon electrode
DPV	Differential pulse voltammetry
E_{acc}	Accumulation potential
E_{clean}	Cleaning potential

E_{dep}	Deposition potential
GCE	Glassy carbon electrode
HMDE	Hanging mercury drop electrode
ICP-MS	Inductively coupled plasma mass spectrometry
ICP-OES	Inductively coupled plasma optical emission spectrometry
LOD	Limit of detection
LOQ	Limit of quantification
ND	Not detected
Q	Quercetin
QSA	Quercetin-5′-sulfonic acid
RSD	Relative standard deviation
SD	Standard deviation
SPE	Screen-printed carbon electrode
SSR	Sum of squared residuals
SWV	Square wave voltammetry
t_{acc}	Accumulation time
TCE	Technologically critical element
t_{clean}	Cleaning time
t_{dep}	Deposition time

References

1. Cobelo-García, A.; Filella, M.; Croot, P.; Frazzoli, C.; Du Laing, G.; Ospina-Alvarez, N.; Rauch, S.; Salaun, P.; Schafer, J.; Zimmermann, S. COST action TD1407: Network on technology-critical elements (NOTICE)—From environmental processes to human health threats. *Environ. Sci. Pollut. Res.* **2015**, *22*, 15188–15194. [CrossRef] [PubMed]
2. Dang, D.H.; Filella, M.; Omanovic, D. Technology-Critical Elements: An Emerging and Vital Resource that Requires more In-depth Investigation. *Arch. Environ. Contam. Toxicol.* **2021**, *81*, 517–520. [CrossRef] [PubMed]
3. Yandem, G.; Jabłońska-Czapla, M. Review of indium, gallium, and germanium as emerging contaminants: Occurrence, speciation and evaluation of the potential environmental impact. *Arch. Environ. Prot.* **2024**, *50*, 84–99. [CrossRef]
4. Keith, L.S.; Maples-Reynolds, N. Germanium. In *Handbook on the Toxicology of Metals*, 5th ed.; Nordberg, G.F., Costa, M., Eds.; Academic Press: Amsterdam, The Netherlands; Elsevier: Amsterdam, The Netherlands, 2022; Volume 2, pp. 289–316.
5. García-Figueroa, A.; Filella, M.; Matoušek, T. Speciation of germanium in environmental water reference materials by hydride generation and cryotrapping in combination with ICP-MS/MS. *Talanta* **2021**, *225*, 121972. [CrossRef] [PubMed]
6. Filella, M.; Matoušek, T. Germanium in Lake Geneva (Switzerland/France) along the spring productivity period. *Appl. Geochem.* **2022**, *143*, 105352. [CrossRef]
7. Filella, M.; Rodríguez-Murillo, J.C. Germanium in the environment: Current knowledge and identification of gaps. *Soil Environ. Health* **2025**, *3*, 100132. [CrossRef]
8. Jablonska-Czapla, M.; Grygoyc, K. Speciation and Fractionation of Less-Studied Technology-Critical Elements (Nb, Ta, Ga, In, Ge, Tl, Te): A Review. *Pol. J. Environ. Stud.* **2021**, *30*, 1477–1486. [CrossRef]
9. Helim, R.; Zazoua, A.; Korri-Youssoufi, H. Sustainable Biopolymer-Based Electrochemical Sensors for Trace Heavy Metal Determination in Water: A Comprehensive Review. *Chemosensors* **2024**, *12*, 267. [CrossRef]
10. Wlazłowska, E.; Grabarczyk, M. Adsorptive Stripping Voltammetry for Determination of Vanadium: A Review. *Materials* **2023**, *16*, 3646. [CrossRef] [PubMed]
11. Wang, J.; Lu, J.; Hocevar, S.B.; Farias, P.A.M.; Ogorevc, B. Bismuth-Coated Carbon Electrodes for Anodic Stripping Voltammetry. *Anal. Chem.* **2000**, *72*, 3218–3222. [CrossRef] [PubMed]
12. Economou, A. Bismuth-film electrodes: Recent developments and potentialities for electroanalysis. *TrAC Trends Anal. Chem.* **2005**, *24*, 334–340. [CrossRef]
13. Xhanari, K.; Finsgar, M. Recent advances in the modification of electrodes for trace metal analysis: A review. *Analyst* **2023**, *148*, 5805–5821. [CrossRef] [PubMed]
14. Grabarczyk, M.; Adamczyk, M. Bismuth film electrode and chloranilic acid as a new alternative for simple, fast and sensitive Ge(IV) quantification by adsorptive stripping voltammetry. *RSC Adv.* **2018**, *8*, 15215–15221. [CrossRef] [PubMed]
15. Krolicka, A.; Zarebski, J.; Bobrowski, A. Catalytic Adsorptive Stripping Voltammetric Determination of Germanium Employing the Oxidizing Properties of V(IV)-HEDTA Complex and Bismuth-Modified Carbon-Based Electrodes. *Membranes* **2021**, *11*, 524. [CrossRef] [PubMed]

16. Grabarczyk, M.; Cwikla-Bundyra, W.; Siewierska, O. The Exploitation of Carbon Nanomaterials as Electrode Material to Increase the Sensitivity of Germanium Ion Determinations by Stripping Adsorption Voltammetry. *Materials* **2026**, *19*, 173. [CrossRef] [PubMed]
17. Rojas, C.; Arancibia, V.; Gómez, M.; Nagles, E. Simultaneous Determination of Antimony(III) and Molybdenum(VI) by Adsorptive Stripping Voltammetry Using Quercetin as Complexing Agent. *Electroanalysis* **2013**, *25*, 439–447. [CrossRef]
18. Rojas, C.; Arancibia, V.; Gómez, M.; Nagles, E. High sensitivity adsorptive stripping voltammetric method for antimony(III) determination in the presence of quercetin-5′-sulfonic acid. Substituent effect on sensitivity. *Sens. Actuators B Chem.* **2013**, *185*, 560–567. [CrossRef]
19. Rojas-Romo, C.; Arancibia, V.; Moreno-da Costa, D.; Tapia, R.A. Highly sensitive determination of vanadium (V) by catalytic adsorptive stripping voltammetry. Substituent effect on sensitivity III. *Sens. Actuators B Chem.* **2016**, *224*, 772–779. [CrossRef]
20. Rojas-Romo, C.; Aliaga, M.E.; Arancibia, V. Determination of molybdenum(VI) via adsorptive stripping voltammetry using an ex-situ bismuth screen-printed carbon electrode. *Microchem. J.* **2020**, *154*, 104589. [CrossRef]
21. Rojas-Romo, C.; Arancibia, V. A Comparative Study of 8-Hydroxyquinoline and 8-Hydroxyquinoline-5-sulfonic Acid for Antimony(III) Determination by AdSV. Substituent Effect on Sensitivity II. *Electroanalysis* **2015**, *27*, 1262–1267. [CrossRef]
22. Escobar-Olivos, D.; González-Ponce, N.; Villalobos, V.; Urzúa, M.; Rojas-Romo, C. Efficient Determination of Se(IV) with a Glassy Carbon Bismuth Film Electrode: Overcoming Cu(II) Interference. *J. Anal. Test.* **2025**, *9*, 250–262. [CrossRef]
23. Papan, P.; Kantapan, J.; Sangthong, P.; Meepowpan, P.; Dechsupa, N. Iron (III)-Quercetin Complex: Synthesis, Physicochemical Characterization, and MRI Cell Tracking toward Potential Applications in Regenerative Medicine. *Contrast Media Mol. Imaging* **2020**, *2020*, 8877862. [CrossRef] [PubMed]
24. Filella, M.; May, P.M. The aqueous solution chemistry of germanium under conditions of environmental and biological interest: Inorganic ligands. *Appl. Geochem.* **2023**, *155*, 105631. [CrossRef]
25. Zhai, G.; Zhu, W.; Duan, Y.; Qu, W.; Yan, Z. Synthesis, characterization and antitumor activity of the germanium-quercetin complex. *Main Group Chem.* **2012**, *35*, 103–109. [CrossRef]
26. Ren, J.; Meng, S.; Lekka, C.E.; Kaxiras, E. Complexation of Flavonoids with Iron: Structure and Optical Signatures. *J. Phys. Chem. B.* **2008**, *112*, 1845–1850. [CrossRef] [PubMed]
27. Corrente, G.A.; Malacaria, L.; Beneduci, A.; Furia, E.; Marino, T.; Mazzone, G. Experimental and theoretical study on the coordination properties of quercetin towards aluminum(III), iron(III) and copper(II) in aqueous solution. *J. Mol. Liq.* **2021**, *325*, 115171. [CrossRef]
28. Panhwar, Q.K.; Memon, S. Synthesis and properties of zirconium(IV) and molybdate(II) morin complexes. *J. Coord. Chem.* **2012**, *65*, 1130–1143. [CrossRef]
29. Torreggiani, A.; Tamba, M.; Trinchero, A.; Bonora, S. Copper(II)–Quercetin complexes in aqueous solutions: Spectroscopic and kinetic properties. *J. Mol. Struct.* **2005**, *744–747*, 759–766. [CrossRef]
30. Pokrovski, G.S.; Schott, J. Thermodynamic properties of aqueous Ge(IV) hydroxide complexes from 25 to 350 °C: Implications for the behavior of germanium and the Ge/Si ratio in hydrothermal fluids. *Geochim. Cosmochim. Acta* **1998**, *62*, 1631–1642. [CrossRef]
31. Lichtfouse, E.; Morin-Crini, N.; Bradu, C.; Boussouga, Y.-A.; Aliaskari, M.; Schäfer, A.I.; Das, S.; Wilson, L.D.; Ike, M.; Inoue, D.; et al. Methods for selenium removal from contaminated waters: A review. *Environ. Chem. Lett.* **2022**, *20*, 2019–2041. [CrossRef]
32. Smedley, P.L.; Kinniburgh, D.G. Molybdenum in natural waters: A review of occurrence, distributions and controls. *Appl. Geochem.* **2017**, *84*, 387–432. [CrossRef]
33. Ungureanu, G.; Santos, S.; Boaventura, R.; Botelho, C. Arsenic and antimony in water and wastewater: Overview of removal techniques with special reference to latest advances in adsorption. *J. Environ. Manag.* **2015**, *151*, 326–342. [CrossRef] [PubMed]
34. Rojas, L.A.; Vizcarra, A.; Hernández-Saravia, L.P. Fabrication of Nanoporous Gold Film: A Novel Electrochemical Sensor for Germanium (II). *Electroanalysis* **2025**, *37*, e202400292. [CrossRef]

Disclaimer/Publisher's Note: The statements, opinions and data contained in all publications are solely those of the individual author(s) and contributor(s) and not of MDPI and/or the editor(s). MDPI and/or the editor(s) disclaim responsibility for any injury to people or property resulting from any ideas, methods, instructions or products referred to in the content.